

# Supporting Information

Aghaallaei et al. 10.1073/pnas.1000467107

## SI Materials and Methods

**Phylogenetic Analyses.** The basic local alignment search tool (BLAST) program available at the Ensembl database site (<http://www.ensembl.org/info/about/species.html>) was used for identification of chemokine receptors in medaka (*O. latipes*) and tetraodon (*T. nigrovirdis*). Initially, human protein sequences were used as query sequences; top-scoring hits were used as second degree query sequences to identify potential paralogues. Phylogenetic relationships were deduced after alignment of protein sequences with programs implemented in the Geneious program (Biomatters). For information on sequences, see [Table S1](#).

**Transgenic Line.** The 5'-upstream region of the *cxcr3a* gene (nt -4 to nt -1,880 from ATG start codon, i.e., nt 18,395,178–18,397,057 of chromosome 16) was amplified by PCR using the DNA amplification kit (Phusion DNA polymerase; New England Biolabs) following manufacturer's protocol. This fragment was cloned into a vector (pSgfp) containing the *gfp* followed by SV40 polyadenylation sequence. The resulting *cxcr3a:gfp* construct is flanked by two I-SceI meganuclease recognition sites. The construct was injected at 20 ng/μL with 0.5 U/μL I-SceI (New England Biolabs) into the blastomere at the one-cell stage. Six embryos exhibiting the strongest GFP expression at 5 dpf were selected for further breeding. Two stable transgenic lines were identified and showed identical GFP expression pattern. F<sub>2/3</sub> transgenic offspring of these fish were used for the experiments.

**Live Microscopy of *cxcr3c:gfp* Fry.** For all movies, medaka fry (10–15 dpf) were anesthetized in 0.01% Tricaine in hatching solution and immobilized in 1% low-melting agarose. Fluorescence microscopy was performed as described previously (1). Movies were evaluated for cell tracking with ImageJ version 1.43g software (National Institutes of Health), using the manual tracking plug-in. For the phagocytosis experiment, the red fluorescence gene (HcRed) was cloned into a pIVEX2.4d vector (Roche) and transformed into BL21 strain (Promega) as described (2). The *E. coli* bacteria suspension was microinjected into fin tissue by using a pressure injector (FemtoJet; Eppendorf).

**Immunohistochemistry.** Paraffin sections (5–7 μm) were deparaffinized, rehydrated, and pretreated with 10 mM sodium citrate

buffer, Tween 20 (pH 6), followed by washes in distilled water and incubation in PBS solution with 0.025% Triton X-100 and normal donkey serum (5% final concentration in PBS solution) to block nonspecific binding. The primary rabbit polyclonal anti-GFP antibody (ab290; Abcam) was used at 1:200 dilution. Specific binding was developed with Cy3-conjugated donkey anti-rabbit antibody at 1:400 dilution. Slides were mounted in Fluoromount-G and DAPI.

**EM.** For ultrastructural analysis of kidney and spleen cells by transmission EM, cells were fixed in 4% paraformaldehyde and 4% glutaraldehyde in buffer (pH 7.2) at 4 °C overnight. After washing with PBS buffer, cells were embedded in 2% agarose and then postfixed with 1% OsO<sub>4</sub> in H<sub>2</sub>O for 1 h on ice, washed with H<sub>2</sub>O, treated with 1% aqueous uranyl acetate for 1 h at 4 °C, dehydrated through a graded series of ethanol, infiltrated with ethanol/resin mixtures, and finally embedded in Epon (with Glycidether 100; Roth). For analysis of blood cells, fixed cells were sucked into cellulose microcapillaries of 200 μm diameter and 2-mm-long capillary tube segments were transferred to aluminum platelets of 150 μm depth containing 1-hexadecene (3). The platelets were sandwiched with platelets without any cavity and then frozen with a high-pressure freezer (Bal-Tec HPM 010; Balzers). The frozen capillary tubes were freed from extraneous hexadecene under liquid nitrogen and transferred to 2-mL microtubes with screw caps containing the substitution medium precooled to -90 °C. Samples were freeze-substituted with an AFS unit (Leica) in 2% osmium tetroxide, 0.5% uranyl acetate (prepared from a 20% stock solution in methanol) in anhydrous acetone at -90 °C for 32 h, warmed to -60 °C within 3 h, kept at -60 °C for 4 h, and warmed to -40 °C within 2 h. After adding 80 μL of an aqueous solution of 25% glutaraldehyde was added, the samples were warmed up to 0 °C. Finally samples were washed with acetone, transferred into an acetone-Epon mixture at room temperature (1:1 for 1 h, 2:1 for 2 h), infiltrated in Epon, and polymerized at 60 °C for 48 h. Ultrathin sections were collected on coated slot grids, stained with uranyl acetate and lead citrate, and viewed in a Philips CM10 electron microscope at 60 kV using a 30-μm objective aperture.

1. Bajoghli B, et al. (2009) Evolution of genetic networks underlying the emergence of thymopoiesis in vertebrates. *Cell* 138:186–197.
2. Rogé J, Betton JM (2005) Use of pIVEX plasmids for protein overproduction in *Escherichia coli*. *Microb Cell Fact* 4:18.

3. Hohenberg H, Mannweiler K, Müller M (1994) High-pressure freezing of cell suspensions in cellulose capillary tubes. *J Microsc* 175:34–43.

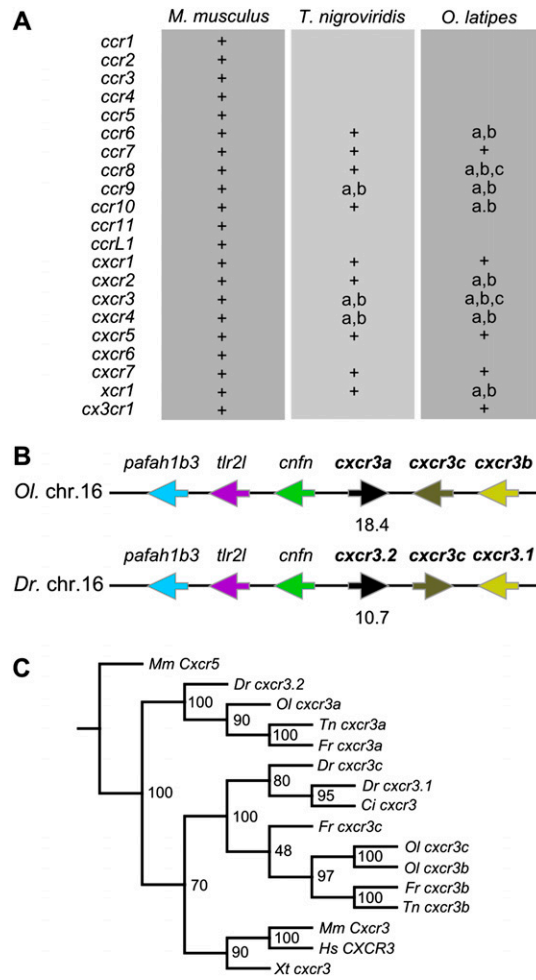


**Fig. S1.** Chemokine receptors in teleost fish. (A) Summary of chemokine receptor genes identified in *T. nigroviridis* and *O. latipes* genomes. (B) Short-range synteny relationships across the *cxc3* gene clusters of *O. latipes* (Ol) and *D. rerio* (Dr). (C). Phylogenetic relationship of *cxc3* paralogs. The fugu genome (1) contains three paralogues of *cxc3* that all are assigned to the same scaffold (Table S1).

1. Brenner S, et al. (1993) Characterization of the pufferfish (Fugu) genome as a compact model vertebrate genome. *Nature* 366:265–268.

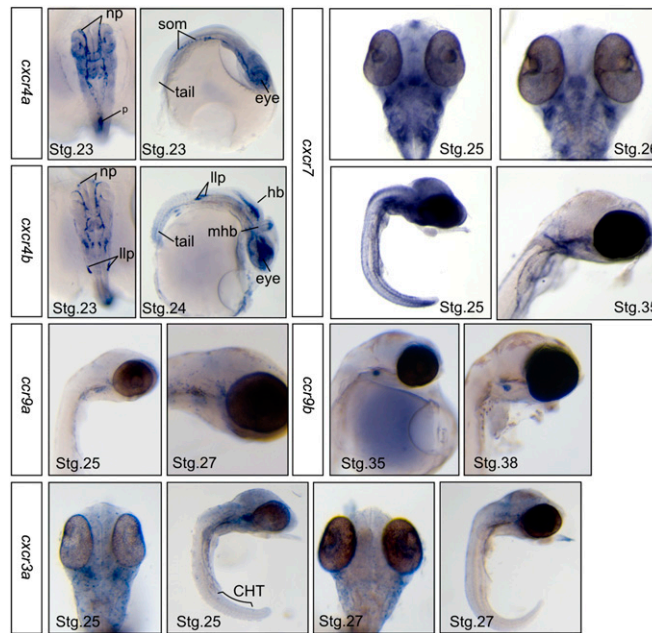


**Fig. S2.** Expression of chemokine receptor genes in medaka embryos at the indicated stages of development (1). np, nasal placode; p, pronephros; som, somites; llp, lateral line primordium; mhb, midbrain-hindbrain boundary; hb, hindbrain; CHT, caudal hematopoietic tissue.

1. Iwamatsu T (2004) Stages of normal development in the medaka *Oryzias latipes*. *Mech Dev* 121:605–618.

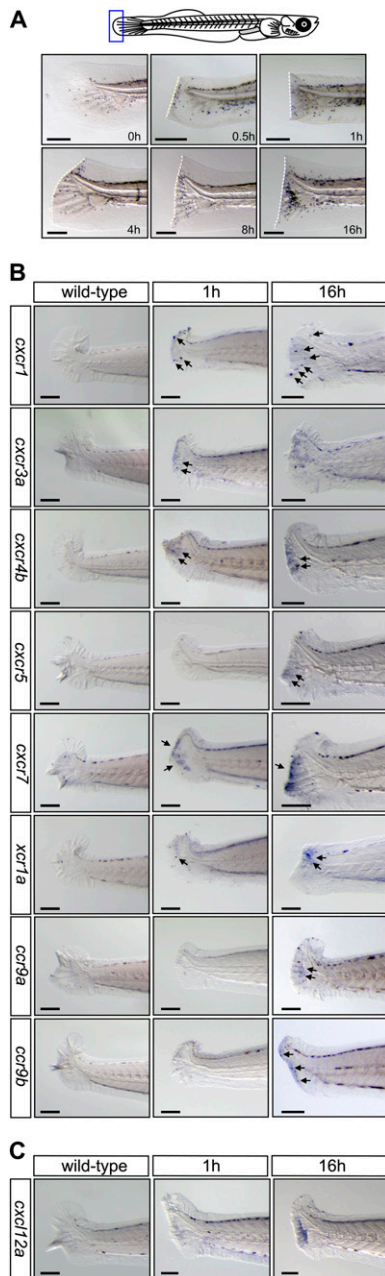


**Fig. S3.** Expression of chemokine receptor genes during the wounding response in *O. latipes* larvae. (A) Time course of the accumulation of Sudan black-positive cells near the wound in the tail fin. (Scale bars, 100  $\mu$ m.) (B) Whole-mount RNA in situ hybridization analysis for chemokine receptor gene expression near the wound in the tail fin. Some of the positive cells are indicated by arrows. (Scale bars, 100  $\mu$ m.) (C) Up-regulation of *cxcl12a*, encoding a ligand of the *cxcr4* and *cxcr7* receptors after wounding. (Scale bars, 100  $\mu$ m.)

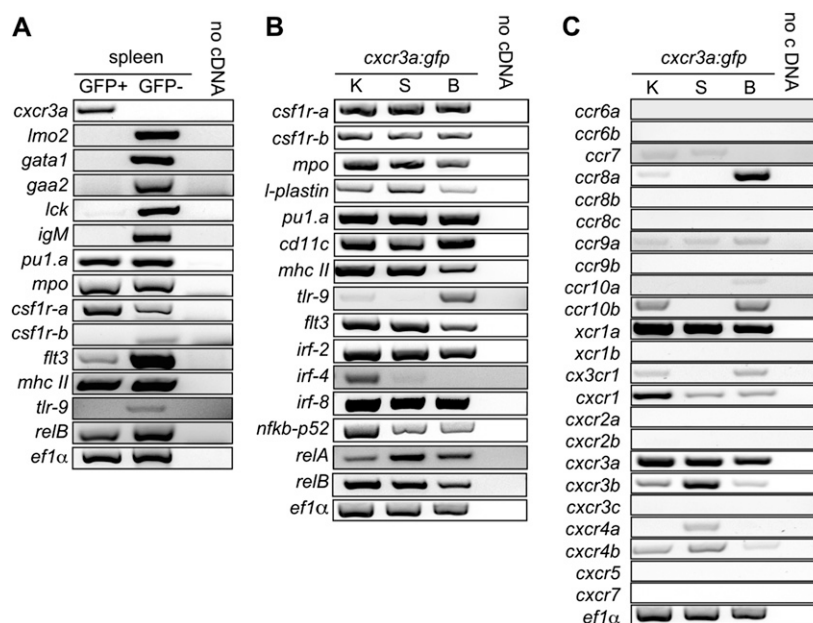


**Fig. 54.** Gene expression profiles. (A) Gene expression patterns of GFP-positive and GFP-negative cells isolated from adult spleen. (B) Comparative expression analysis of GFP-positive cells isolated from different tissues of adult fish. (C) Expression of chemokine receptor genes in GFP-positive cells isolated from different tissues of adult fish.

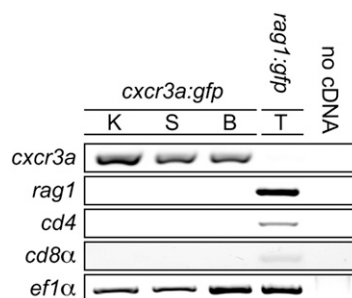


**Fig. 55.** GFP-positive cells of embryos lack expression of specific T-cell markers. As a positive control, GFP-positive cells from a *rag1:gfp* line (1) were used.

- Li J, Iwanami N, Hoa VQ, Furutani-Seiki M, Takahama Y (2007) Noninvasive intravital imaging of thymocyte dynamics in medaka. *J Immunol* 179:1605–1615.

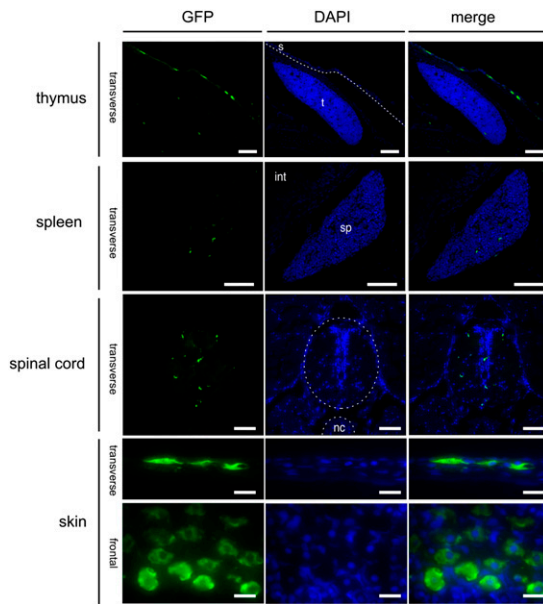


**Fig. S6.** Tissue distribution of GFP-positive cells. The distribution of GFP-positive cells was analyzed by immunofluorescence analysis in sections of thymus, spleen, spinal cord, and skin of adult fish. Nuclei were stained with DAPI. S, skin; t, thymus; int, intestine; sp, spleen; nc, notochord. (Scale bars, 100  $\mu\text{m}$  for thymus, spleen, spinal cord; 5  $\mu\text{m}$  for skin.)

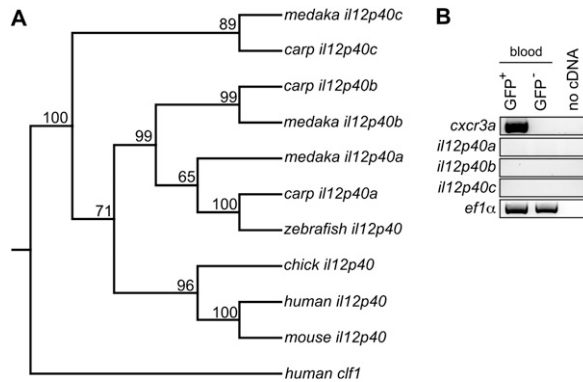
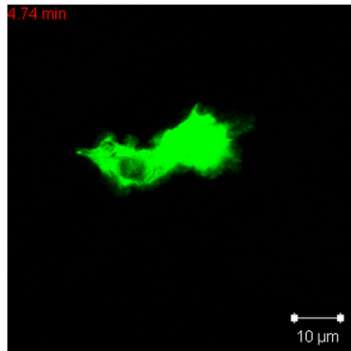
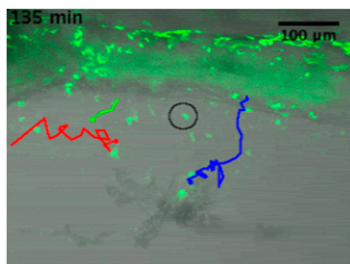


**Fig. S7.** Three paralogues of *il12p40* exist in medaka. (A) Phylogenetic tree based on derived protein sequences of *il12p40* genes of human, mouse, chicken, carp, zebrafish, and medaka genomes. The sequence for the human CLF1 was used as an outgroup. (B) Expression of *il12p40* paralogs is undetectable in GFP-positive and GFP-negative blood cells of naive *cxcr3a:gfp* transgenic animals.



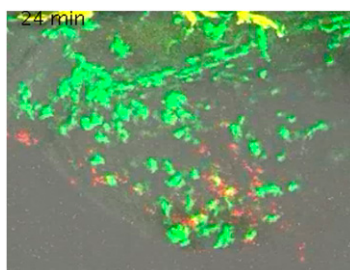
**Movie S1.** A motile *cxcr3a*-expressing cell in transgenic larvae.

[Movie S1](#)



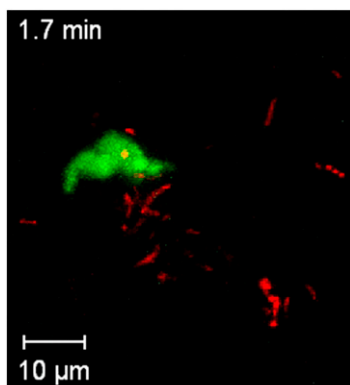
**Movie S2.** Response of *cxcr3a*-expressing cells to wounding of transgenic larvae. The wounded site can be recognized as a somewhat darker tissue at the lower edge of the fin. Note the different migratory behaviors of individual cells; some tracks are highlighted with tracking software.

[Movie S2](#)



**Movie S3.** Clearance of bacteria (red fluorescence) in transgenic larvae, at least partly owing to phagocytosing *cxcr3a*-expressing cells (yellow fluorescence). The yellow fluorescence at the top of the frame emanates from autofluorescent pigment cells.

[Movie S3](#)



**Movie S4.** A motile phagocytosing *cxcr3a*-expressing cell in transgenic larvae; bacteria are red fluorescent.

[Movie S4](#)

## Other Supporting Information Files

[Table S1 \(DOC\)](#)

[Table S2 \(DOC\)](#)